Indian Journal of Biochemistry & Biophysics
Vol. 62, January 2025, pp. 78-87
DOI: 10.56042/ijbb.v62i1.12810

Zinc Oxide Nanorods from *Prunus domestica* L.: Bio-Assisted Synthesis, Characterization, Antioxidant and Cytotoxic Activities

Kishan[1]*, Rishi Kumar Shukla[1]* & Abha Shukla[2]

[1]Department of Chemistry, Gurukula Kangri (Deemed to be University), Haridwar-249 404, Uttarakhand, India

[2]Department of Chemistry, Kanya Gurukula Campus, Gurukula Kangri (Deemed to be University), Haridwar-249 404, Uttarakhand, India

Received 28 July 2024; *revised 10 September 2024*

The unique characteristics and extraordinary features of nanotechnology and nanoscience are making them the next big, rapidly expanding fields. Nowadays, there is a lot of interest in bio-assisted synthesis as a way to get beyond the limits of physical and chemical methods. In the present work, we synthesized the zinc oxide nanorods (ZnONRs) using a methanolic extract of the seed coats of *Prunus domestica* L., which are regarded as PDMeOH-ZnONRs. Standard characterization techniques (UV-Vis, FTIR, XRD and FE-SEM) were used to examine the morphological properties of the synthesized PDMeOH-ZnONRs. The UV-Vis spectrum has shown the SPR peak between 311 – 351 nm confirming the synthesis of PDMeOH-ZnONRs. The fourier transform infrared spectroscopy (FTIR) spectrum revealed the presence of different functional groups like hydroxyl, amine, nitrile, nitro, carboxyl, esters *etc.* in the fabricated PDMeOH-ZnONRs. The X-ray diffraction (XRD) analysis confirmed the wurtzite hexagonal structure. The diameter of PDMeOH-ZnONRs ranged from 42.373 ± 9.109 nm, which is confirmed by the field emission scanning electron microscope (FE-SEM) technique. The PDMeOH-ZnONRs exhibited excellent 2,2-diphenyl-1-picrylhydrazyl (DPPH) inhibitory activity with an IC_{50} value of 31.700 ± 1.239 µg/mL. The PDMeOH-ZnONRs have shown outstanding hydrogen peroxide (H_2O_2) scavenging activity with an IC_{50} value of 33.126 ± 0.717 µg/mL. Further, the cytotoxicity of the PDMeOH-ZnONRs was checked by brine shrimp lethality assay (BSLA) and *3-(4,5-dimethylthiazol-2-yl)-2,5-diphenyltetrazolium bromide* (MTT) assay, which showed LC_{50} value of 91.336 ± 3.784 mg/L and IC_{50} value of 174.240 ± 0.460 µg/mL, respectively. Overall findings indicate that the PDMeOH-ZnONRs synthesized *via* green route have good biological potentials and might be employed in future biomedical applications.

Keywords: PDMeOH-ZnONRs, UV-Vis, FTIR, XRD, FE-SEM, DPPH, H_2O_2, BSLA, MTT

Nanotechnology has grown tremendously during the last few decades because of its applications in the field of medicine, chemistry and biotechnology. Progress in this field has created intriguing possibilities in nanoscience, notably in drug delivery, gene delivery, nanomedicine and biosensing[1]. Nanoparticles (NPs) are tiny, multipurpose particles ranging from 1 to 100 nm in diameter[2]. Owing to their high surface area-to-volume ratio and unique physicochemical characteristics, including colour, dispersion and thermodynamics, the NPs exhibit size-related characteristics that set them apart from bulk materials and give them distinctive features when compared to their macroscale counterparts[3].

Zinc is an essential trace element that is present in muscle, bone, skin and hard tissues of the teeth[4]. The Zinc oxide (ZnO) is being utilized in sunscreens and other personal care products due to its strong UV absorption capabilities[5].

With a molecular weight of 81.38 g/mol, zinc oxide nanoparticles (ZnONPs) are a colourless, odourless white powder. It is regarded by the FDA as a generally recognized as safe (GRAS) material[4]. The ZnONPs have undergone extensive research due to their appealing characteristics such as biocompatibility, eco-friendliness, low cost, ease of fabrication, high photosensitivity, large excitation binding energy, high thermal conductivity and stability under harsh environmental conditions[6]. Due to the distinct useful characteristics, the ZnONPs are widely employed in a variety of disciplines, including electronics, optics, food packaging, cosmetic goods, petroleum industries, medicines and agriculture. Aside from these uses, the ZnONPs are frequently used in biological applications such as anticancer, antibacterial, antioxidant, anti-inflammatory, wound healing and drug delivery[7]. Furthermore, the ZnONPs are well-known as an excellent photocatalyst agent,

Correspondence:
E-mail: prajapati75kishan@gmail.com (KP); and
rkshukla@gkv.ac.in (RKS)

providing a potential option for waste water treatment[8].

Multifunctional properties of the ZnO enable it to grow into a variety of morphologies, such as 1-D (rods, tubes, wires, *etc*.), 2-D (disks, sheets, plates, *etc*.) and 3-D (particles, flowers, *etc*.) nanostructures. These morphologies are primarily dependent on chemical precursors, supplementary usage of capping (*i.e.*, stabilizing) agent (such as plant extract), high temperature and pressure conditions[9]. The crystal structure of zinc oxide nanorods (ZnONRs) is wurtzite, formed by hexagonal sub-lattices of one particular kind of atom interpenetrating each other tightly. The ZnONRs have a binding energy of 60 eV and a band-gap of around 3.3 eV. The higher mechanical and chemical stability of the ZnO is due to its wurtzite structure[10].

Recently, plant extract-derived formulated metal and metal oxide NPs have been investigated as potential substitute of bio-control agents[2]. Numerous studies on the production of plant-mediated metal-based NPs have been published as a result of widespread distribution the phytochemicals in various plant parts, including flowers, fruits, stems, leaves and roots[11,12]. Several variables are known to influence the synthesis and characteristics of the NPs, such as the kind of plant extract utilized, pH of the medium, degree of concentration of metal salt, interaction time and temperature[13].

Prunus domestica L. (also known as plum) is an important medicinal plant of Rosaceae family. Its fruit is used as food and medicine, which is eaten either fresh or dried. Consumption of the fruit of *P. domestica* is associated with many therapeutic benefits such as improvement blood circulation, measles and digestive disorders[14]. The primary polyphenolic components in *P. domestica* are chlorogenic acids, anthocyanins, flavanols, flavonols and coumarins. Many studies reveals that the fruit of *P. domestica* exhibits several remarkable pharmacological activities such as antioxidant, antihyperlipidemic, anticancer, anti-osteoporosis, anxiolytic, antibacterial and memory enhancing properties[15].

Since the fruit of *P. domestica* is juicy and fleshy that people often consume fresh, the seeds and seed coats are thrown away. Thus, keeping the above advantages of *P. domestica* in view, the current study is mainly focused on the green synthesis of ZnONRs using the methanolic extract of the seed coats. The antioxidant activity (by DPPH and H_2O_2 scavenging assays) and cytotoxic activity (by brine shrimp lethality and MTT assays) of ZnONRs are also studied in the present work. Additionally, there could be a host of health advantages linked to the seed coats.

Materials and Methods

Sample collection and authentication

The fruits of *P. domestica* were bought from the neighbourhood orchards situated in Haridwar, Uttarakhand (India). The plant was identified and authenticated by Botanical Survey of India (BSI), Dehradun.

Chemicals and reagents

Petroleumether (SD fine), diethyl ether (SD fine), ethyl acetate (SD fine), methanol (CDH), 2,2-diphenyl-1-picrylhydrazyl (DPPH) (Alpha acer), ascorbic acid (Merck), zinc acetate dihydrate (Fisher), DMSO (CDH), KH_2PO_4 (CDH) and K_2HPO_4 (CDH). All other reagents which were used in this study were of analytical grade.

Extract preparation

The extraction was performed according to Mohan *et al.*, (2021) with a few alterations[16]. Briefly, 200 g of the powder of the seed coats was placed into the thimble of Soxhlet extractor. Approximately 72 cycles of the siphoning were conducted with methanol (after petroleum ether, diethyl ether and ethyl acetate, respectively) or the procedure was continued till the siphoning tube appeared colourless. Particulate material was eliminated *via* filtering the extract. Using a rotary evaporator, under reduced pressure, the extract was concentrated and the concentrated extracts were kept refrigerated till further analysis.

Zinc oxide nanorods using the methanolic extract of seed coats of *P. domestica* (*i.e.*, PDMeOH-ZnONRs)

The synthesis of PDMeOH-ZnONRs was performed as described by Kumar *et al.*, (2024) with some modifications[17]. Zinc acetate dihydrate [$Zn(OAc)_2.2H_2O$] was employed as the precursor for the synthesis of PDMeOH-ZnONRs. In brief, 13 g of $Zn(OAc)_2.2H_2O$ was dissolved in 100 mL of 0.6 M MeOH. To this, 400 mg of methanolic extract of the seed coats of *P. domestica* was incorporated and stirred for 3 h. The resultant solution was filtered through Whatmann filter paper number 40 and the filtrate was titrated with 10% NH_3 solution till the precipitation was over. To get rid of the excess ammonia, the precipitates were filtered and then washed with hot water. The precipitates were baked at

105°C for a whole night to dry them out. Then, the dried precipitates were calcined for 4 h at 400°C.

Characterization of synthesized PDMeOH-ZnONRs

The synthesis of PDMeOH-ZnONRs was confirmed by recording the absorption spectrum using a UV-Vis-NIR spectrophotometer (Shimadzu, UV-3600) at resolution of 0.5 nm. The presence of the various functional groups of the plant extract was revealed by recording the FTIR spectrum in a range of 400-4000 cm^{-1} (Perkin Elmer, FTIR spectrum version 10.4.00) by KBr pellet method. The crystal structural analysis of the PDMeOH-ZnONRs was done by the powder X-ray diffraction (p-XRD) pattern recorded on X-ray diffractometer (Panalytical X-Pert Pro) in continuous scan type mode from 5° to 100° of 2θ. The size morphology of the PDMeOH-ZnONRs was characterized by field emission-scanning electron microscopy (FE-SEM Supra 55, Karl Zeiss).

Antioxidant Activity

2,2-diphenyl-1-picrylhydrazyl (DPPH) free radical scavenging assay

The PDMeOH-ZnONRs were evaluated for their antioxidant potential as describe by Brand-William *et al.*, (1995) and Ali *et al.*, (2021) by the DPPH method with some modifications[10,18]. Briefly, 1mL of the PDMeOH-ZnONRs at different concentrations (5, 10, 15, 20, 25, 50 and 100 µg/mL in DMSO) was mixed with 3 mL of DPPH (0.004% *w/v* solution in methanol) and incubated at room temperature for 30 min. After 30 min, the resultant mixture was centrifuged at 12000 rpm for 3 min and the absorbance of supernatant was measured at 517 nm using a double beam UV-Vis spectrophotometer (Systronics - 2205). The colour shift from pink to yellow signifies that the sample under examination has been scavenging the DPPH free radicals. Ascorbic acid was used as standard. 1 mL of solvent and 3 mL of DPPH solution served as blank. The % inhibition of DPPH was calculated by the following equation:

$$\%\ \text{inhibition} = \frac{\text{Absorbance of the blank} - \text{Absorbance of the sample}}{\text{Absorbance of the blank}} \times 100$$

Hydrogen peroxide (H_2O_2) scavenging activity

The antioxidant activity of the PDMeOH-ZnONRs was tested by hydrogen peroxide scavenging assay (*i.e.,*H_2O_2method) also[19]. A solution of H_2O_2 (40 mM) was freshly prepared in 0.05 M KH_2PO_4-K_2HPO_4 phosphate buffer (pH = 7.4). The PDMeOH-ZnONRs at various concentrations (5, 10, 15, 20, 25 and 50 µg/mL) were mixed with 1.4 mL phosphate buffer and 0.6 mL 40 mM H_2O_2 and vortexed. After 10 min, the resulting solution was centrifuged and concentration of the H_2O_2 in the supernatant was determined at 230 nm by a UV-Vis spectrophotometer (Systronics - 2205). Ascorbic acid was used as the positive control. In a similar manner, the blank experiment was also conducted. All the tests were performed in triplicate. The % H_2O_2 scavenging was calculated by the following formula:

$$\%\ \text{H2O2 scavenging} = \frac{\text{Absorbance of the blank} - \text{Absorbance of the sample}}{\text{Absorbance of the blank}} \times 100$$

Cytotoxic activity

Brine shrimp lethality assay (BSLA)

The BSLA was performed as described by Khan *et al.*, (2021) with some modifications[20]. To hatch the shrimp eggs, 36 g of sea salt was dissolved in 1 L of distilled water in order to make artificial seawater. A hatching chamber, a little plastic container with a lid to separate the sections for light and dark, was filled with seawater. Shrimp eggs were put in the dark side of the chamber and the lamp above the side that had been lit will draw the shrimp that have hatched. For two days, the shrimp were left to hatch and develop into nauplii (or larvae). When the shrimp larvae were ready (two days later), 15 brine shrimps were placed into the test tube containing 5 mL of artificial seawater along with 5 mL of the PDMeOH-ZnONRs solution (10, 50 and 100 mg/L). In the same manner, control experiment was also performed using 1% DMSO in artificial sea water for negative control experiment and doxorubicin for positive control experiment. After 24 h, the number of shrimps that survived was counted. The % mortality was calculated by the following formula:

$$\%\ \text{mortality} = \frac{\text{Number of the dead nauplii}}{\text{Total number of the nauplii}} \times 100$$

This is to make sure that whether the substances in the nanorods (NRs) are the cause of the nauplii's death (mortality) or not.

***3-(4,5-dimethylthiazol-2-yl)-2,5-diphenyltetrazolium bromide* (MTT) assay**

The cytotoxicity of the PDMeOH-ZnONRs was determined by *3-(4,5-dimethylthiazol-2-yl)-2,5-*

*diphenyltetrazolium bromide (*MTT) assay as described by Alam *et al.*, (2024) against lever (HepG-2) cell line with some modifications[21]. HepG-2 cells were grown in 96 well plates and incubated for 24 h in a humified environment at 37°C. Then, the cells were treated with the PDMeOH-ZnONRs at various concentration (10, 50, 100, 150 and 200 µg/mL) containing a final volume of 100 µL/well. After 24 h of incubation the cells were labelled with 10 µL MTT solution and again incubated at 37°C for 24 h. Finally, the absorbance was recorded using micro-plate reader after dissolving the formazan crystals in 120 µL of DMSO at 570 nm. DMSO was used as negative control and doxorubicin was used as positive control. The cell viability was calculated by the following formula:

$$\% \text{ cell viability} = \frac{\text{Absorbance of treated cells}}{\text{Absorbance of control cells}} \times 100$$

Results and Discussion

Characterization of synthesized PDMeOH-ZnONRs

Ultra violet-visible (UV-Vis) spectroscopy

The colour of the reaction mixture altered from brown to pale yellow during the synthesis process, suggesting the formation of PDMeOH-ZnONRs. The UV-Vis spectrum of the PDMeOH-ZnONRs was recorded between 200-800 nm. (Fig. 1) shows the UV-Vis spectrum of the biosynthesized PDMeOH-ZnONRs. The UV-Vis spectrum showed the surface plasmon resonance (SPR) peak of the ZnO between 311-351 nm and has shown the absorption maxima at 350.5 nm. Which is consistent with the previously reported study reporting the SPR peak between 360-380 nm[22]. The methanolic extract from the seed coat of *P. domestica* comprising the bioactive compounds, first converted the Zn^{2+} ions to zero-valent Zn atoms. The residual Zn^{2+} ions are then reduced to the ZnO by the zero-valent Zn atoms, a cluster structure is eventually produced, resulting in the production of the PDMeOH-ZnONRs. For the synthesis of stable nanomaterials, the phytochemicals serve as capping and stabilizing agents[23]. The strong UV absorbance of the biosynthesised ZnONPs indicates their suitability for UV protection applications[24]. The energy band gap (Ebg) of the PDMeOH-ZnONRs is found to be 3.54 eV, which was determined using the equation[25]:

$$Ebg = \frac{1240}{\lambda} (\text{eV})$$

Where, λ represents wavelength (nm) at which the maximum absorption occurred. The Ebg of the ZnONPs using *Sambucus ebulus* extract is reported to be 3.3 eV[24]. In another study, the ZnONPs synthesized using *Cassisa fistula* and *Peltophorum pterocarpum* leaf extract reported the Ebg to be 3.33 and 3.39 eV, respectively[26,27]. Therefore, the obtained results of UV-Vis spectroscopy are in good agreement with the previously reported studies.

Fourier transformation infrared (FTIR) spectroscopy

The different functional groups of plant extract involved in the synthesis (*i.e.*, stabilizing and reduction) of the PDMeOH-ZnONRs were observed using the FTIR method. The FTIR spectrum of the PDMeOH-ZnONRs is shown in (Fig. 2). Various band at 3431.84 cm^{-1} (O-H stretching of carboxylic acid or phenol), 2924.65 (C-H stretching of alkyl group), 2341.81 (CN stretching nitrile), 1709.86

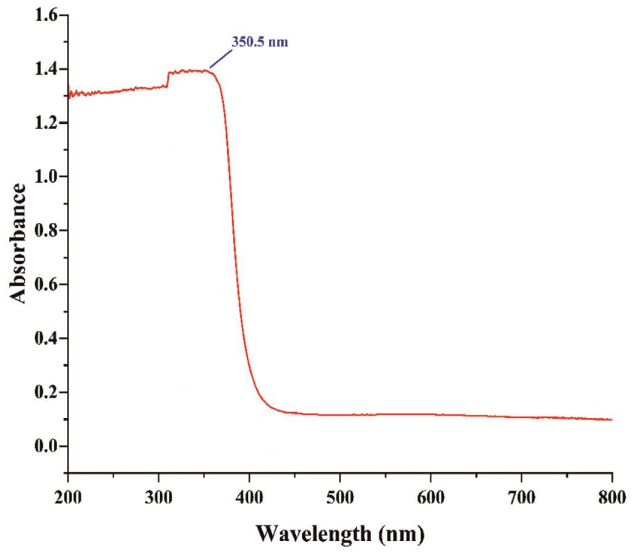

Fig. 1 — UV-Vis spectrum of PDMeOH-ZnONRs

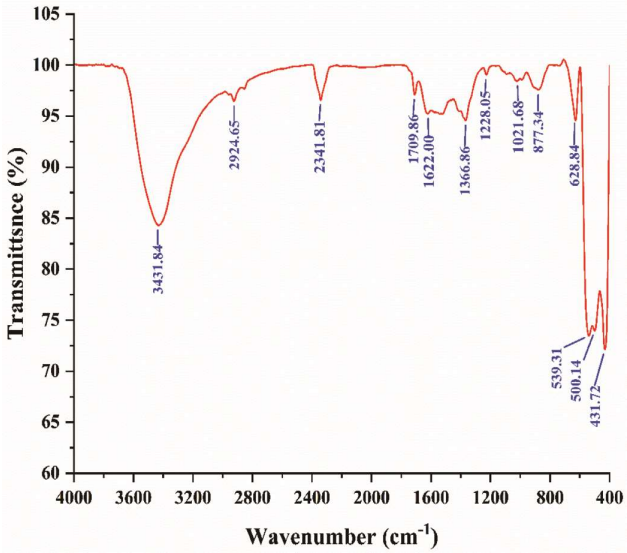

Fig. 2 — FTIR spectrum of PDMeOH-ZnONRs

(C=O of stretching), 1622.00 (N-H bending of amide or amines), 1366.86 (N-O stretch of nitro compound or weak C-H rocking of alkane), 1228.05 (C-N stretch of amine), 1021.68 (C-O stretch of alcohol, carboxyl or ether), 877.34 (out of plane N-H bending vibrations amine), 628.84, 539.31 500.14 and 431.72 (metal oxide or Zn-O vibrations) are evident in the FTIR spectrum of the PDMeOH-ZnONRs[2,24,27-30]. Consequently, these distinct bands suggest that an array of biomolecules present in the extract of seed coats of *P. domestica* were crucial in the reduction and stability of the PDMeOH-ZnONRs [31].

The use of natural plant extract in the synthesis of the NPs has several benefits. One such benefit is that the NPs may be coated with various pharmacological entities (such as phenolic and polyphenolic phytochemicals) on the metal oxide layer[24]. Carboxylic, amino and phenolic acids play a crucial role in bio-capping during the synthesis and interact with the surface of the ZnONPs and contribute to the stability of the generated ZnONPs[2]. Which helps the NPs to link with their recipients on bacterial membranes[24].

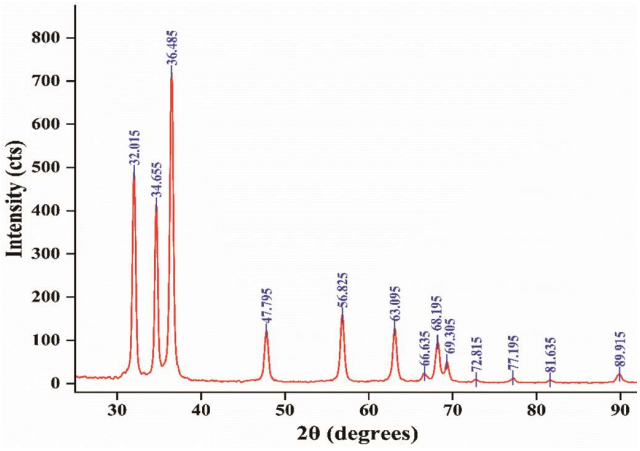

Fig. 3 — XRD pattern of PDMeOH-ZnONRs

X-ray diffractometry (XRD)

The XRD pattern of the PDMeOH-ZnONRs is demonstrated in (Fig. 3) and provides a strong insight of their crystalline structure. Table 1 demonstrates the miller indices (hkl), full width half maxima (FWHM), peak position, relative peak area and crystallite size of the PDMeOH-ZnONRs. There are distinct diffraction peaks at 2θ values of 32.015, 34.655, 36.485, 47.795, 56.825, 63.095, 66.635, 68.195, 69.305, 72.815, 77.195, 81.635 and 89.915 degrees. The corresponding miller indices of these peaks *i.e.*, diffraction lattice planes are (100), (002), (101), (102), (110), (103), (200), (112), (201), (004), (202), (104) and (203), respectively. Which confirms the hexagonal wurtzite structure of the bio synthesized PDMeOH-ZnONRs. The XRD pattern matches with the Joint Committee on Powder Diffraction Standards (JCPDS) card no. 96-210-7060. Using the Debye–Scherer equation, the average crystallite size of the PDMeOH-ZnONRs was determined as following[17,32]:

$$D = \frac{K\lambda}{\beta Cos\theta}$$

Where, D = Crystallite size, λ = X-ray wavelength coming from Cu-K_α (0.1540560 nm), θ = Bragg's diffraction angle, K = Shape factor or Scherrer constant (0.89), β = full width at half maxima of the diffraction peak in radians.

Field emission-scanning electron microscopy (FE-SEM)

Figure 4 represents the two FE-SEM images (A and B) of the PDMeOH-ZnONRs. It is apparent from

Table 1 — Miller indices, FWHM, relative peak area and average crystallite size of PDMeOH-ZnONRs

Miller indices (hkl)	FWHM	Peak position (2θ in degrees)	Relative peak area	Crystallite size (nm)
100	0.464	32.015	310.96	17.619
002	0.431	34.655	280.35	19.105
101	0.478	36.485	475.75	17.326
102	0.542	47.795	105.70	15.852
110	0.537	56.825	125.57	16.648
103	0.551	63.095	103.31	16.722
200	0.909	66.635	25.92	10.349
112	0.608	68.195	66.71	15.621
201	0.603	69.305	38.61	15.843
004	0.747	72.815	8.97	13.073
202	0.610	77.195	9.80	16.492
104	0.658	81.635	4.90	15.773
203	0.761	89.915	20.00	14.597
Average crystallite size				15.771 ± 2.184 nm

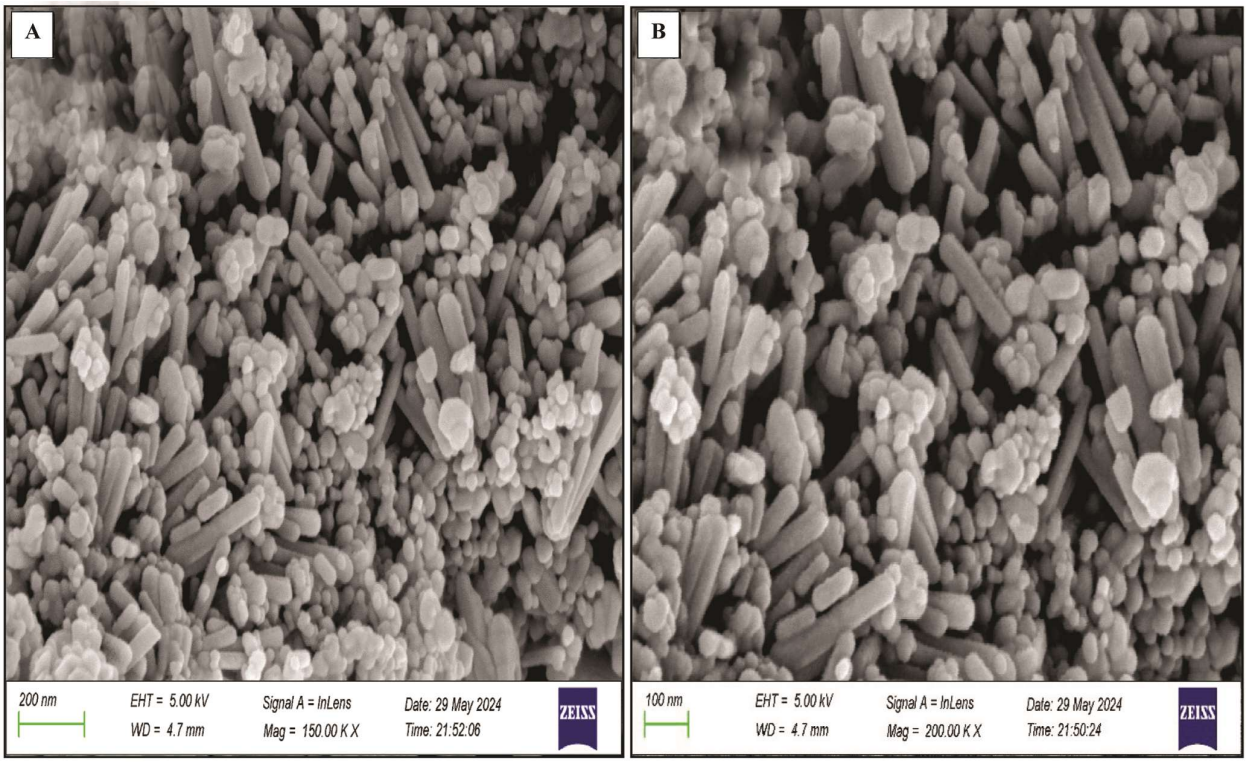

Fig. 4 — FE-SEM images of PDMeOH-ZnONRs

the (Fig. 4) that the PDMeOH-ZnONRs have the rod like shape. The average diameter of the PDMeOH-ZnONRs by FE-SEM is measured to be 42.373 ± 9.109 nm with the help of ImageJ software. The XRD analysis clarifies the overall morphology of the PDMeOH-ZnONRs to be hexagonal wurtzite nanorods. Shape plays a vital role in the pathogenicity of the NPs. In a previous study for oral drug delivery, it has been demonstrated that, in comparison to spherical particles, rod-shaped particles have greater cellular absorption and transit across intestinal cells indicating that the effectiveness of the NPs in oral drugs administration may be potentially enhanced by the rod-shaped NPs[33]. In addition to this, due to its remarkable applicability in a wide range of sectors, including solar cells, sensors, photodetectors, photocatalysts, sensors and spatial microchip technology, the ZnONRs have been the subject of substantial research[34].

Antioxidant activity

2,2-diphenyl-1-picrylhydrazyl (DPPH) free radical scavenging assay

One of the simplest and most used methods for determining antioxidant activity is the DPPH method. The hydrogen atom from the antioxidant molecule reduces the unpaired valence electron on the nitrogen atom in the DPPH radical. Consequently, DPPH-H hydrazine is generated[35]. The amount of quenched DPPH radicals can be estimated by spectrophotometric measurements by examining the absorbance drop between 515 and 520 nm[36]. The results of the DPPH free radical scavenging assay are depicted in (Table 2). Figure 5 depicts the variation of % inhibition of DPPH against the concentration. The PDMeOH-ZnONRs and standard (*i.e.*, ascorbic acid), both have shown a dose dependant response. The results of the DPPH assay are demonstrated in terms of IC_{50} value (*i.e.*, concentration for the 50% scavenging of DPPH free radicals)[37]. The IC_{50} value of the PDMeOH-ZnONRs is found to be 31.700 ± 1.239 µg/mL, while the IC_{50} value of ascorbic acid is found to be 14.035 ± 0.043 µg/mL. In a previous study, the ZnONPs fabricated *via* aqueous extract of the seeds of *Caesalpinia crista* demonstrated concentration-dependent antioxidant activity by the DPPH method, which is consistent with our

Table 2 — DPPH scavenging assay of PDMeOH-ZnONRs

Sample	IC_{50} (µg/mL)
PDMeOH-ZnONRs	31.700 ± 1.239
Ascorbic acid (standard)	14.035 ± 0.043

Each experiment was performed in triplicate. Values are represented as mean ± SD.

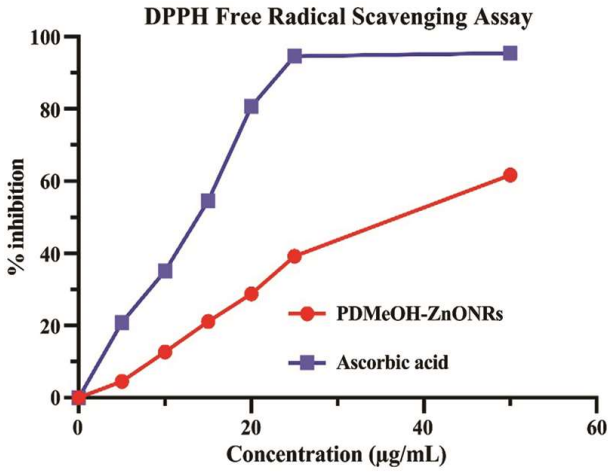

Fig. 5 — Variation of % inhibition of DPPH against concentration

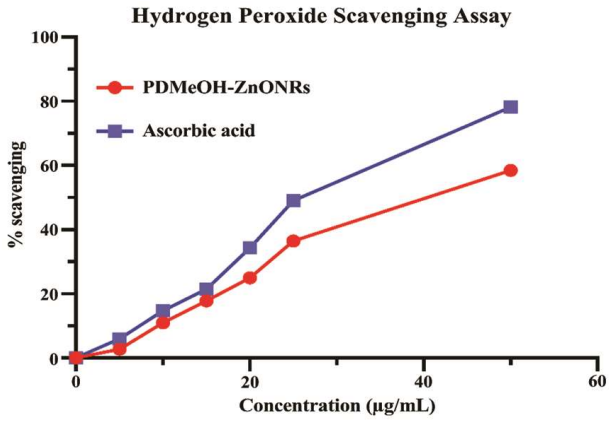

Fig. 6 — Variation of % scavenging of hydrogen peroxide against concentration

Table 3 — H_2O_2scavenging assay of PDMeOH-ZnONRs

Sample	IC_{50} (µg/mL)
PDMeOH-ZnONRs	33.126 ± 0.717
Ascorbic acid (standard)	25.352 ± 0.138

Each experiment was performed in triplicate. Values are represented as mean ± SD

Table 4 — Brine shrimp lethality assay of PDMeOH-ZnONRs

Sample	IC_{50} (mg/L)
PDMeOH-ZnONRs	91.336 ± 3.784
Doxorubicin (standard)	30.152 ± 0.755

Each experiment was performed in triplicate. Values are represented as mean ± SD

findings[38]. The PDMeOH-ZnONRs exhibit remarkable results because of their high surface area and colloidal behavior[10].

Hydrogen peroxide (H_2O_2) scavenging assay

Hydrogen peroxide scavenging is one of the most important method to assess the antioxidant activity. Although hydrogen peroxide is not very reactive by itself, it occasionally poses a hazard to cells due to its potential to produce hydroxyl radicals within the cells[39]. Therefore, H_2O_2 removal is critical for antioxidant defence in dietary or cell systems[40]. The results of the H_2O_2 free radical scavenging assay are depicted in (Table 3). The variation of % scavenging of H_2O_2 against the concentration is shown in (Fig. 6). The results of H_2O_2 scavenging activity are again expressed in terms of IC_{50} value. The IC_{50} value of the PDMeOH-ZnONRs is 33.126 ± 0.717 µg/mL, whereas the IC_{50} value of the ascorbic acid is found to be 25.352 ± 0.138 µg/mL. From the Figure 6, it can be clearly seen that the PDMeOH-ZnONRs have shown the dose dependant response along with the ascorbic acid.

Cytotoxic activity

Brine shrimp lethality assay (BSLA)

The lethality concentrations of the PDMeOH-ZnONRs used were 10, 50 and 100 mg/L. The lethality was directly proportional to the sample concentration. The lowest lethality was observed at a concentration of 10 mg/L which was 11.11 ± 3.85%. The BSLA results are depicted in (Table 4). Figure 7 depicts the variation of % mortality against the concentration. The LC_{50} value of the PDMeOH-ZnONRs is found to be 91.336 ± 3.784 mg/L, while the LC_{50} of doxorubicin (standard) is found to be 30.152 ± 0.755 mg/L. The BSLA results are generally reported using several criteria, as follows: A material is considered extremely hazardous if its LC_{50} value is less than 1.0 mg/L; it is considered toxic if its LC_{50} value is between 1.0 and 10.0 mg/L; moderately toxic compounds have an LC_{50} value between 10.0 and 30.0 mg/L; mildly toxic compounds have an LC_{50} value between 30.0 and 100.0 mg/L; and non-toxic compounds have an LC_{50} > 100.0 mg/L[41]. Thus, the results indicate that the PDMeOH-ZnONRs and doxorubicin, both have shown the mild toxicity towards brine shrimp larvae, however, PDMeOH-ZnONRs are less toxic than doxorubicin. In a previously published report, the lethality of the ZnONPs was also dose dependant, which is consistent with present study[22].

***3-(4,5-dimethylthiazol-2-yl)-2,5-diphenyltetrazolium bromide* (MTT) assay**

The MTT test is based on measuring mitochondrial activity by forming formazan crystals from MTT using live cells. This test is frequently employed to

Table 5 — MTT assay of PDMeOH-ZnONRs

Sample	IC_{50} (µg/mL)
PDMeOH-ZnONRs	174.240 ± 0.460
Doxorubicin (standard)	148.450 ± 0.924

Each experiment was performed in triplicate. Values are represented as mean ± SD

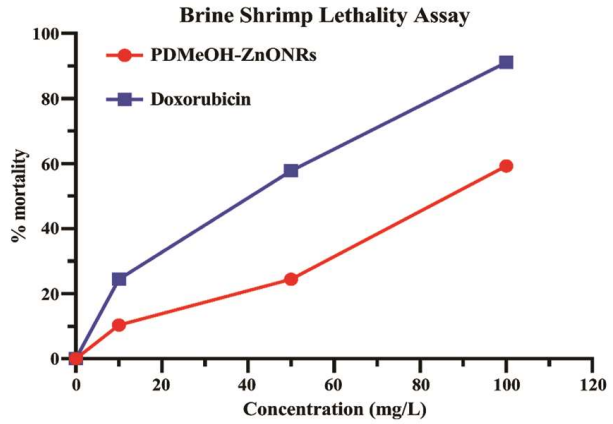

Fig. 7 — Variation of % mortality against concentration

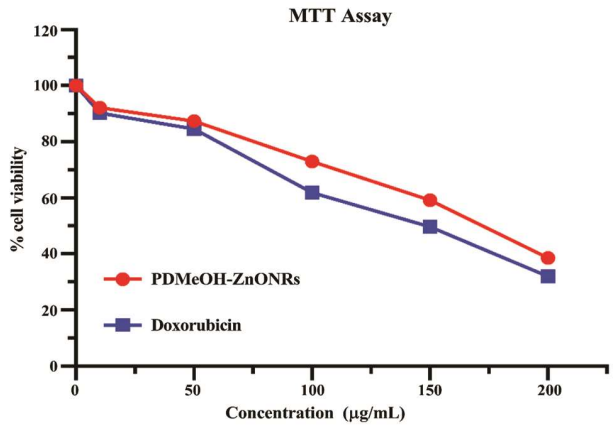

Fig. 8 — Variation of % cell viability against concentration

evaluate the cytotoxic effects of medicines/cancer drugs on cell lines. Since the number of viable cells is associated with overall mitochondrial activity in the vast majority of cell populations[42]. The results of MTT assay are depicted in (Table 5). The results of MTT assay demonstrate the PDMeOH-ZnONRs as potent inhibitor of HepG-2 cell proliferation. Here again the results are expressed in terms of IC_{50}. Figure 8 represents the % cell viability against the concentration. The PDMeOH-ZnONRs have shown an IC_{50} value of 174.240 ± 0.460 µg/mL, while the doxorubicin has shown the IC_{50} value of 148.450 ± 0.924 µg/mL. In this study, the PDMeOH-ZnONRs have shown a dose dependent response, *i.e.*, HepG-2 cell proliferation decreased as the concentration of the PDMeOH-ZnONRs increased. In a previous MTT study carried on MCF-7 cell lines, the cell proliferation decreased as the dose of the ZnONPs increase, which is consistent with our srudy[43]. When employed to deliver and load hydrophobic anti-cancer medicines, the ZnONPs demonstrates extraordinary behaviour due to their low toxicity towards 3T3 fibroblast cells. In addition to this, higher uptake of the ZnONPs by the cancerous cells is responsible for the greater cytotoxicity towards the cancerous cells[44,45]. Thus, the results of the present study demonstrated the importance of synthesized PDMeOH-ZnONRs in drug delivery applications also.

Conclusion

Researchers are currently concentrating on developing environmentally sustainable methods for producing the ZnONPs for a range of therapeutic applications. Green synthesized ZnONPs are widely appreciated since they are less expensive, biocompatible and have less of an adverse influence on the environment than those made by chemical and physical means. A good source for the sustainable production of the ZnONPs is the diversity of phytochemicals found in plant extracts, including flavonoids, polyphenols, terpenoids, alkaloids and tannins. By using this process, the stability of the ZnONPs is increased and novel physicochemical features may be explored. The current study has demonstrated that the NPs synthesized using the methanolic extract of the seed coats of *P. domestica* have acquired the rod like shape, which have high intestinal absorption capacity in comparison to sphere like nano materials. The PDMeOH-ZnONRs are found to be excellent antioxidant agents because they have shown strong DPPH radical scavenging activity along with good H_2O_2 scavenging activity. The PDMeOH-ZnONRs have also shown the amazing results of cytotoxic activity by BSLA and MTT methods. Therefore, it is a hot topic of research because of great potential for application in the biological and pharmacological domains. Hence, we believe that the pharmacological and biological domains may make use of the PDMeOH-ZnONRs.

Acknowledgement

Authors are extremely thankful to Department of Chemistry, GK(DU), Haridwar, Uttarakhand for providing experimental facilities. Kishan is also thankful to Material Research Centre *(*MRC*)* at Malaviya National Institute of Technology (MNIT),

Jaipur, Rajasthan and Central Building Research Institute (CBRI), Council of Scientific and Industrial Research (CSIR), Roorkee for carrying out the FTIR, XRD and FE-SEM analyses.

Conflicts of interest

The authors declare that they do not have any conflicts of interest to declare.

References

1 Jayachandran A, Aswathy TR & Nair AS, Green synthesis and characterization of zinc oxide nanoparticles using *Cayratia pedata* leaf extract. *Biochem Biophys Rep*, 26 (2021) 100995.

2 Ifeanyichukwu UL, Fayemi OE & Ateba CN, Green synthesis of zinc oxide nanoparticles from pomegranate (*Punica granatum*) extracts and characterization of their antibacterial activity. *Molecules*, 25 (2020) 4521.

3 Zhou XQ, Hayat Z, Zhang DD, Li MY, Hu S, Wu Q, Cao YF & Yuan Y, Zinc oxide nanoparticles: synthesis, characterization, modification and applications in food and agriculture. *Processes*, 11 (2023) 1193.

4 Baek M, Chung HE, Yu J, Lee JA, Kim TH, Oh JM, Lee WJ, Paek SM, Lee JK, Jeong J & Choi SJ, Pharmacokinetics, tissue distribution and excretion of zinc oxide nanoparticles. *Int J Nanomed*, 7 (2012) 3081.

5 Newman MD, Stotland M & Ellis JI, The safety of nanosized particles in titanium dioxideand zinc oxide based sunscreens. *J Am Acad Dermatol*, 61 (2009) 685.

6 Mohammadi FM & Ghasemi N, Influence of temperature and concentration on biosynthesis and characterization of zinc oxide nanoparticles using cherry extract. *J Nanostruct Chem*, 8 (2018) 93.

7 Saravanan M, Gopinath V, Chaurasia MK, Syed A, Ameen F & Purushothaman N, Green synthesis of anisotropic zinc oxide nanoparticles with antibacterial and cytofriendly properties. *MicrobPathog*, 115 (2018) 57.

8 Roshitha SS, Mithra V, Saravanan V, Sadasivam SK & Gnanadesigan M, Photocatalytic degradation of methylene blue and safranin dyes using chitosan zinc oxide nano-beads with *Musa×paradisiaca* L. pseudo stem. *BioresourTechnol Rep*, 5 (2019) 339.

9 Suresh S, Thambidurai S, Arumugam J, Kandasamy M, Pugazhenthiran N, Balaji D, Al-Asbahi BA, Reddy NR, Kumar AA & Muneeswaran T, Antibacterial activity and photocatalytic oxidative performance of zinc oxide nanorods biosynthesized using *Aervalanata* leaf extract. *Inorg Chem Commun*, 139 (2022) 109398.

10 Ali S, Sudha KG, Karunakaran G, Kowsalya M, Kolesnikov E & Rajeshkumar MP, Green synthesis of stable antioxidant, anticancer and photocatalytic activity of zinc oxide nanorods from *Leea asiatica* leaf. *J Biotechnol*, 329 (2021) 65.

11. Adeyemi JO, Elemike EE & Onwudiwe DC, ZnO nanoparticles mediated by aqueous extracts of *Dovyalis caffra* fruits and the photocatalytic evaluations. *Mater Res Express*, 6 (2019) 125091.

12 Husen A, Nanoscience and plant–soil systems. In: gold nanoparticles from plant system: synthesis characterization and their application, Cham: Springer, (2017).

13 Li X, Xu H, Chen ZS & Chen G, Biosynthesis of nanoparticles by microorganisms and their applications. *J Nanomater*, 2011 (2011) 270974.

14 Ahmed T, Sadia H, Khalid A, Batool S & Janjua A, Prunes and liver function: a clinical trial. *Pak J Pharmaceu Sci*, 23 (2010) 463.

15 Sultana N, Rehman H, Muntaha ST, Haroon Z, Fatima D & Fakhra H, *Prunus domestica*: a review. *Asian J Pharmacog*, 4 (2020) 21.

16 Mohan E, Suriya S, Shanmugam S & Rajendran K, Qualitative phytochemical screening of selected medicinal plants. *J Drug Deliv Ther*, 11 (2021) 141.

17 Kumar S, Bithel N, Kumar S, Kishan, Sen M & Banerjee C, Phyto-mediated synthesis of zinc oxide nanoparticles from *Clerodendrum infortunatum* L. leaf extract and evaluation of antibacterial potential. *S Afr J Bot*, 164 (2024) 146.

18 Brand-William W, Cuvelier ME & Berset CLWT, Use of a free radical method to evaluate antioxidant activity. *LWT-Food Sci Technol*, 28 (1995) 25.

19 Baali N, Khecha A, Bensouici A, Speranza G & Hamdouni N, Assessment of antioxidant activity of pure graphene oxide (GO) and ZnO-decorated reduced graphene oxide (rGO) using DPPH radical and H_2O_2 scavenging assays. *Carbon*, 5 (2019) 75.

20. Khan AK, Renouard S, Drouet S, Blondeau JP, Anjum I, Hano C, Abbasi BH & Anjum S, Effect of UV irradiation (A and C) on *Casuarina equisetifolia*-mediated biosynthesis and characterization of antimicrobial and anticancer activity of biocompatible zinc oxide nanoparticles. *Pharmaceutics*, 13 (2021) 1977.

21 Alam MF, Amjad I, Saadullah M, Tahir M, Jawad M, Asif M, Atif M, Zara S & Rashad M, Antitumor activity of zinc oxide nanoparticles fused with green extract of *Nigella sativa*. *J Saudi Chem Soc*, 28 (2024) 101814.

22 Wahab A, Waqas M, Urooj S, Tariq H, Abbasi ZY, Ali M & Abbasi BH, Synthesis of zinc oxide nanoparticles (ZnONPs) from leaf extract of *Carthamus oxycantha* and its *in vitro* biological applications. *Austin J Anal Pharm Chem*, 10 (2023) 1159.

23 Basnet P, Chanu TI, Samanta D & Chatterjee S, A review on bio-synthesized zinc oxide nanoparticles using plant extracts as reductants and stabilizing agents. *J Photochem Photobiol Biol*, 183 (2018) 201.

24 Alamdari S, Ghamsari MS, Lee C, Han W, Park HH, Tafreshi MJ, Afarideh H & Ara MHM, Preparation and characterization of zinc oxide nanoparticles using leaf extract of *Sambucus ebulus*. *Appl Sci*, 10 (2020) 3620.

25 Arakha M, Roy J, Nayak PS, Mallick B & Jha S, Zinc oxide nanoparticle energy band gap reduction triggers the oxidative stress resulting into autophagy-mediated apoptotic cell death. *Free Radica Biol Med*, 110 (2017) 42.

26 Suresh D, Nethravathi PC, Rajanaika H, Nagabhushana H & Sharma SC, Green synthesis of multifunctional zinc oxide (ZnO) nanoparticles using *Cassia fistula* plant extract and their photodegradative, antioxidant and antibacterial activities. *Mater Sci Semicond Proc*, 31 (2015) 446.

27 Pai S, Sridevi H, Varadavenkatesan T, Vinayagam R & Selvaraj R, Photocatalytic zinc oxide nanoparticles synthesis using *Peltophorum pterocarpum* leaf extract and their characterization. *Optik*, 185 (2019) 248.

28 MuthuKathija M, Badhusha MSM & Rama V, Green synthesis of zinc oxide nanoparticles using *Pisonia Alba* leaf extract and its antibacterial activity. *Appl Surf Sci Adv*, 15 (2023) 100400.

29 Pavia DL, Lampman GM, Kriz GS & Vyvyan JR, Spectroscopy, (2011) 8th Indian Reprint.

30 Naseer M, Aslam U, Khalid B & Chen B, Green route to synthesize zinc oxide nanoparticles using leaf extracts of *Cassia fistula* and *Melia azadarach* and their antibacterial potential. *Sci Rep*, 10 (2020) 9055.
31 Padalia H, Moteriya P & Chanda S, Synergistic antimicrobial and cytotoxic potential of zinc oxide nanoparticles synthesized using *Cassia auriculata* leaf extract. *Bionanoscience*, 8 (2018) 196.
32 Essalah G, Leroy G, Carru JC, Duponchel B, Mascot M, Poupin C, Cousin R, Guermazi S & Guermazi H, Conduction mechanisms and relaxation phenomena along with electronic transition of $ZnO/ZnNb_2O_6/Nb_2O_5$ composite. *Ceram Int*, 47 (2021) 24732.
33 Banerjee A, Qi J, Gogoi R, Wong J & Mitragotri S, Role of nanoparticle size, shape and surface chemistry in oral drug delivery. *J Control Release*, 238 (2016) 176.
34 Aspoukeh PK, Barzinjy AA & Hamad SM, Synthesis, properties and uses of ZnO nanorods: a mini review. *Int Nano Lett*, 12 (2022) 153.
35 Sirivibulkovit K, Nouanthavong S & Sameenoi Y, Paper-based DPPH assay for antioxidant activity analysis. *Anal Sci*, 34 (2018) 795.
36 Dawidowicz AL, Wianowska D & Olszowy M, On practical problems in estimation of antioxidant activity of compounds by DPPH method (Problems in estimation of antioxidant activity). *Food Chem*, 131 (2012) 1037.
37 Semerci AB, İnceçayir D, Konca T, Tunca H & Tunç, K, Phenolic constituents, antioxidant and antimicrobial activities of methanolic extracts of some female cones of gymnosperm plant. *Indian J Biochem Biophys*, 57(2020) 298.
38 Donga S & Chanda S, *Caesalpinia crista* seeds mediated green synthesis of zinc oxide nanoparticles for antibacterial, antioxidant and anticancer activities. *Bionanoscience*, 12 (2022) 451.
39 Halliwell B, Reactive oxygen species in living systems: source, biochemistry, and role in human disease. *AmJMed*, 91 (1991) S14.
40 Keser S, Celik S, Turkoglu S, Yilmaz O & Turkoglu I, Hydrogen peroxide radical scavenging and total antioxidant activity of hawthorn. *Chem J*, 2 (2012) 9.
41 Meer B, Aandleeb A, Iqbal J, Ashraf H, Meer K, Ali JS, Drouet S, Anjum S, Mehmood A, Khan T, Ali M, Hano C & Abbasi BH, Bio-assisted synthesis and characterization of zinc oxide nanoparticles from *Lepidium sativum* and their potent antioxidant, antibacterial and anticancer activities. *Biomolecules*, 12 (2022) 855.
42 Sathelly K, Kumar KN, Kiranmayi MU, Obul RPC & Poda S, Anticancer potential of *Solanum lycopersicum* L. extract in human lung epithelial cancer cells A549. *Indian J Biochem Biophys*, 60 (2022) 76.
43 Deekala V, Babu BK & Rudraraju R, Pharmacological studies of zinc oxide nanoparticles. *Indian J Biochem Biophys*, 56 (2019) 500.
44 Ramakrishnan G, Razack SA, Ravi L & Sahadevan R, Fabrication of phyco-functionalized zinc oxide nanoparticles and their *in vitro* evaluation against bacteria and cancer cell line. *Indian J Biochem Biophys*, 60 (2023) 770.
45 Viswanath KV, Kumar KN, Nagaraj A, Rao KV, Kiranmayi MU, Potla DC & Poda S, *Hibiscus tiliaceus* mediated phytochemical reduction of zinc oxide nanoparticles and demonstration of their antibacterial, anticancer, and dye degradation capabilities. *Indian J Biochem Biophys*, 59 (2022) 565.